Experimental demonstration of GFDM-OFDM hybrid modulation in an IM-DD system

Shaohua An, Lei Han, Qingming Zhu, Ciyuan Qiu and Yikai Su[*]

State Key Laboratory of Advanced Optical Communication Systems and Networks, Department of Electronic Engineering, Shanghai Jiao Tong University, 800 Dongchuan Rd, Shanghai, China, 200240

ABSTRACT

A GFDM-OFDM hybrid modulation scheme is experimentally demonstrated in a 60-Gb/s IM-DD system. 1.9-dB and 3.1-dB receiver sensitivity improvements are achieved compared to the conventional GFDM and OFDM signals in the back-to-back case, respectively.

Keywords: modulation, IMDD, GFDM, OFDM, receiver sensitivity

1. INTRODUCTION

Driven by the tremendous growth of bandwidth-hungry applications such as 4K/8K videos and cloud services, the capacity demands in data center networks have increased rapidly in recent years[1]. In such short-reach scenarios, intensity-modulation direct-detection (IMDD) systems are desired, owing to their advantages of low cost and low power consumption.

However, due to the limited analog bandwidths of electronic components in the IMDD systems, severe inter symbol interference (ISI) is introduced to the transmitted signal in the time domain, while the electrical signal to noise ratio (ESNR) in the high frequency at the receiver decreases in the frequency domain. Moreover, the anti-alias filter in the digital-to-analog converter (DAC) further reduces the ESNR in the high frequency, leading to a degraded bit error ratio (BER) performance of the system[2]. In order to mitigate the high-frequency fading effect, orthogonal frequency division multiplexing (OFDM) can be adopted, due to its robustness to frequency selective fading[3]. However, the high peak-to-average power ratio (PAPR) is a major drawback of the OFDM signal, which limits the modulation efficiency[2]. To reduce the PAPR of the signal while maintaining the robustness to high-frequency fading, various schemes have been proposed, such as the quadrature amplitude modulation-discrete multi-tone (QAM-DMT) technique[4] and the pulse amplitude modulation-discrete multi-tone (PAM-DMT) technique[5]. Nonetheless, these techniques need additional discrete Fourier transform (DFT) and inverse discrete Fourier transform (IDFT) at the transmitter and the receiver respectively, resulting in increased complexities.

In this paper, we experimentally demonstrate a generalized frequency division multiplexing (GFDM)-OFDM hybrid modulation scheme in an IM-DD system, which was proposed and numerically studied in [6] to overcome the inherent high PAPR of the OFDM signal. GFDM is a flexible multicarrier modulation format, which possesses a time-frequency data structure that each GFDM block contains a few subcarriers and multiple sub-symbols per subcarrier, thus has a low PAPR[7]. By allocating a GFDM signal to the low-frequency subcarriers while the high-frequency subcarriers are occupied by an OFDM signal, a novel GFDM-OFDM hybrid modulation can be obtained with both the advantages of low PAPR and robustness to high-frequency fading. Therefore, the block structure of the GFDM signal and the bandwidth ratio between the two signals are crucial, which were comprehensively investigated in our previous simulations[6]. After the previous numerical comparisons, the feasibility of the GFDM-OFDM scheme is further experimentally demonstrated in this paper. In our experiment, 1.9-dB and 3-dB receiver sensitivity improvements are achieved in a 60-Gb/s IMDD system, compared to the conventional GFDM and OFDM signals in the back-to-back case, respectively.

2. OPERATION PRINCIPLE

Fig. 1 shows the digital signal processing (DSP) flow charts at the transmitter side and the receiver side. At the transmitter, the input binary serial data is firstly converted to the parallel format, which is then mapped into QAM constellations. After Hermitian symmetry operation, the generated constellations are sent into a GFDM modulator or an OFDM modulator. In the GFDM modulator, each GFDM block d consists of $K \times M$ symbols, which can be divided into K subcarriers with M sub-symbols in each subcarrier. Let $d = (d_0[0], ..., d_0[M-1], d_1[0], ..., d_{K-1}[M-1])^T$ be the GFDM block, with $d_k[m]$ being the data of the m-th subsymbol in the k-th subcarrier[8]. After inverse fast Fourier transform (IFFT), pulse shaping and circular convolution operation, the output vector $\mathbf{x} = (x[n])^T$ can be expressed as follows[9].

$$x[n] = \sum_{m=0}^{M-1} \sum_{k=0}^{K-1} d_k[m] g[(n-mK) \bmod MK] e^{j2\pi\frac{kn}{K}}, \; n=0, \ldots, MK-1$$

where n is the sampling index and $g[n]$ is a prototype filter performing a modulo operation. As for the OFDM modulator, IFFT is performed to convert the signal from the frequency domain to the time domain, which is similar to the operation applied to the GFDM sub-signal. After adding cyclic prefixes (CP), the generated GFDM sub-signal and the OFDM sub-signal are added to generate a desired GFDM-OFDM signal. At the receiver, synchronization is firstly performed, then a single-tap equalizer is used to compensate linear distortions. Subsequently, a digital filter separates the two sub-signals, following the CP removal for each sub-signal. The recovered two sub-signals are fed into a GFDM demodulator and an OFDM demodulator respectively. In the OFDM demodulator, FFT is implemented to recover the QAM constellations. An additional zero-forcing (ZF) filter is used in the GFDM modulator to remove the inter-carrier interference (ICI) induced by the non-orthogonality[10]. After de-mapping and parallel-to-serial (P/S) conversion, the binary data is retrieved to calculate the BER.
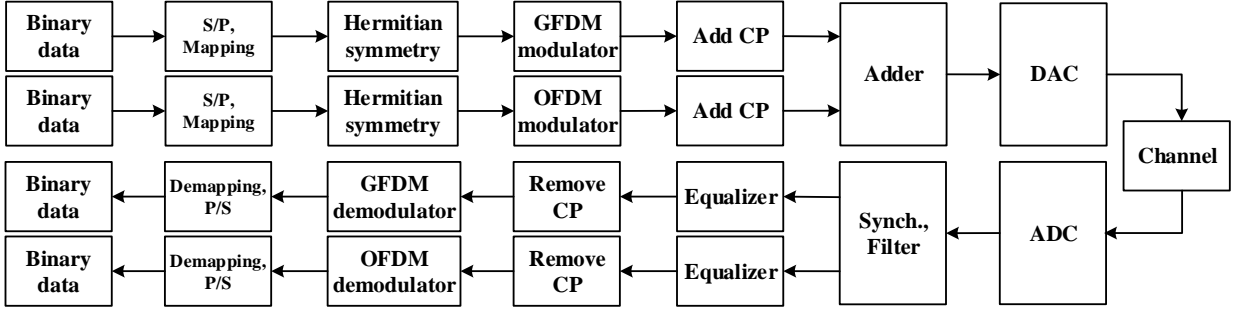

Fig. 1. DSP flow charts. S/P: serial-to-parallel conversion; Synch.: synchronization.

3. EXPERIMENTAL SETUP AND RESULTS

To verify the feasibility of the GFDM-OFDM scheme, a proof-of-concept experiment is performed in an IMDD system, as shown in Fig. 2. The original digital data is generated offline in Matlab, which is then converted to an electrical signal by an arbitrary waveform generator (AWG) (Keysight M8195A), with a 60-GSa/s sampling rate and a 25-GHz analog bandwidth. After amplified by a 45-GHz electrical amplifier (EA), the electrical signal is used to drive a 25-GHz intensity modulator (IM). A continuous wave light from a distributed feedback (DFB) laser at 1550 nm is fed into the IM, which is biased at the quadrature point. After electrical-to-optical (E/O) conversion, the optical signal is attenuated by a variable optical attenuator (VOA) to measure BER curves. At the receiver, the received optical signal is firstly amplified by an
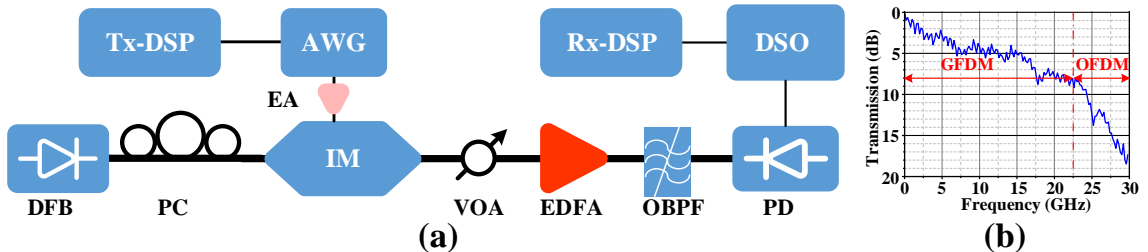

Fig. 2. (a) Experimental setup. (b) Frequency response of the system. PC: polarization controller.

erbium-doped fiber amplifier (EDFA), and then filtered by an optical band-pass filter (OBPF) to mitigate the amplified spontaneous emission (ASE) noise. Using a 40-GHz photodetector (PD), the detected optical signal is converted to an electrical signal, which is subsequently captured by a 36-GHz digital storage oscilloscope (DSO) (LeCroy 36Zi-A) at 80 GSa/s. Finally, the offline DSP is performed to retrieve the binary data and calculate the BER. The frequency response of the system is measured by performing the frequency sweeping of the AWG, as illustrated in Fig. 2(b).

In order to comprehensively compare the GFDM-OFDM hybrid modulation scheme with the conventional GFDM format and OFDM format, we provide a parameter table, Table 1, based on the measured frequency response in Fig. 2(b). For fair comparisons, we set the three signals with the same total symbol number and the same QAM order, thus the same data rate. The total symbol number of the GFDM-OFDM signal is $K_1{\times}M{+}K_2$, where K_1 and K_2 are the subcarrier numbers occupied by the GFDM sub-signal and the OFDM sub-signal respectively. N is the total subcarrier number and M is the sub-symbol number per subcarrier of the GFDM signal. In the experiment, N = 16 and M = 16 are used. The valid signal bandwidth is 30 GHz, with the occupied bandwidths for the two sub-signals are 0~22.5 and 22.5~30 GHz. The raw data rate of the system is 60 Gb/s ($60{\times}\frac{16{\times}2}{32}$).

Table 1. Parameters used in the experiment.

Parameter	GFDM-OFDM	Conventional GFDM	Conventional OFDM
QAM order	4QAM	4QAM	4QAM
Sub-symbols per subcarrier (M)	M	M	M
Subcarriers in the low-frequency sub-signal (K_1)	¾*N	¾*N	¾*N*M
Subcarriers in the high-frequency sub-signal (K_2)	¼*N*M	¼*N	¼*N*M
CP length (N_{cp})	N*M/16	N*M/16	N*M/16
Filter type	Raised cosine	Raised cosine	---
Roll-off factor	0.1	0.1	---

The BER curves of the GFDM-OFDM signal, the GFDM signal and the OFDM signal in the back-to-back case are plotted in Fig. 3, respectively. At the BER threshold of 2×10^{-3}, –21.3-dBm and –20.1-dBm sensitivities are observed for the conventional GFDM signal and the conventional OFDM signal, respectively. The receiver sensitivity of the GFDM-OFDM signal is –23.2 dBm, thus achieving 1.9-dB and 3.1-dB sensitivity improvements compared to the conventional GFDM and OFDM signals, respectively. Constellation diagrams of the investigated signals measured at the –23.2-dBm received power are presented in the insets (i-iii), where the GFDM-OFDM constellation diagram exhibits the best performance, owing to the advantages of both low PAPR and robustness to high-frequency fading.
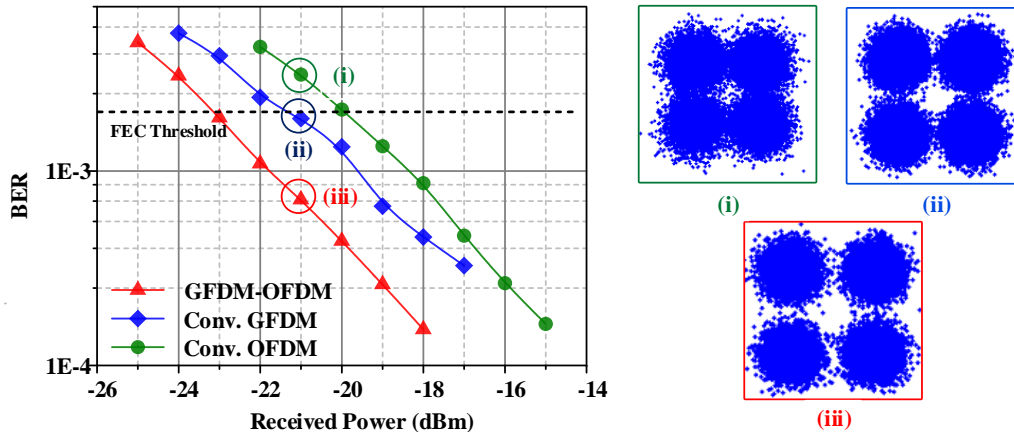
Fig. 3. BER curves of the GFDM-OFDM signal, the GFDM signal and the OFDM signal in the back-to-back case. Insets (i-iii) show the constellations measured at the –23.2-dBm received power

4. CONCLUSION

In this paper, we experimentally demonstrated a novel GFDM-OFDM hybrid modulation scheme, which possesses both low PAPR and robustness to high-frequency fading. In a 60-Gb/s IMDD system, 1.9-dB and 3.1-dB receiver sensitivity improvements are experimentally demonstrated compared to the conventional GFDM and OFDM signals in the back-to-back case, respectively. The results show that the GFDM-OFDM hybrid modulation scheme is a promising technique in short-reach and bandwidth-limited IMDD applications.

The authors hope this manuscript be accepted as an oral presentation.

REFERENCES

[1] Cisco Global Cloud Index: Forecast and Methodology, 2016–2021 White Paper.

[2] J. Peng, S. An, Q. Zhu, C. Qiu, Y. Zhang, and Y. Su, "Sensitivity Improvement in IM-DD OFDM-PON by Amplitude Scaling and Subcarrier Enabled PAPR Reduction," in Proc. CLEO, STh1O.3 (2017).

[3] Meng-Han Hsieh and Che-Ho Wei, "Channel estimation for OFDM systems based on comb-type pilot arrangement in frequency selective fading channels," IEEE Transactions on Consumer Electronics 44(1), 217-225 (1998).

[4] W. A. Ling, I. Lyubomirsky, R. Rodes, H. M. Daghighian, and C. Kocot, "Single-channel 50G and 100G discrete multitone transmission with 25G VCSEL technology," J. Light. Technol. 33(4), 761–767 (2015).

[5] W. A. Ling, Y. Matsui, H. M. Daghighian, and I. Lyubomirsky, "112 Gb/s transmission with a directly-modulated laser using FFT-based synthesis of orthogonal PAM and DMT signals," Opt. Express 23(15), 19202-19212 (2015).

[6] L. Han, S. An, Q. Zhu, C. Qiu and Y. Su, "GFDM-OFDM Hybrid Modulation Scheme for IM-DD Optical Communication Systems," Proc. CONTROLO, 114-119 (2018).

[7] N. Michailow, M. Matthé, I. Gaspar, A. Caldevilla, L. Mendes, A. Festag, and G. Fettweis, "Generalized Frequency Division Multiplexing for 5th Generation Cellular Networks," IEEE Trans. Commun. 62(9), 3045–3061 (2014).

[8] A. Farhang, N. Marchetti, and L. E. Doyle, "Low-Complexity Modem Design for GFDM," IEEE Trans. Signal Process. 64(6), 1507–1518 (2016).

[9] M. Matthé, L. Mendes, I. Gaspar, N. Michailow, D. Zhang, and G. Fettweis, "Precoded GFDM transceiver with low complexity time domain processing," EURASIP J. Wirel. Commun. Netw. 1–9 (2016).

[10] S. K. Antapurkar, A. Pandey, and K. K. Gupta, "GFDM performance in terms of BER, PAPR and OOB and comparison to OFDM system," Proc. AIP 1715, 20039-1-20039-11.